Astron. Astrophys. 327, 219–223 (1997)

ASTRONOMY AND ASTROPHYSICS

The polarimetric orbit of Z Andromedae⋆

H.M. Schmid[1,2] **and H. Schild**[1]

[1] Institut für Astronomie, ETH-Zentrum, CH-8092 Zürich, Switzerland,
[2] Landessternwarte Heidelberg-Königstuhl, D-69117 Heidelberg, Germany

Received 27 February 1997 / Accepted 4 April 1997

Abstract. Repeated Raman line polarimetry of the Z And symbiotic system shows that both the percent polarization, and the polarization angle, are locked to the binary motion. It is thus possible to determine the otherwise unobservable system inclination and orbit orientation on the celestial sphere. We find an inclination of $i = 47 \pm 12°$ and an orbit orientation $\Omega = 72 \pm 6°$. Inserting the inclination in the previously known mass function yields a most likely mass of the stellar hot component of about 0.65 $M_\odot$ which is typical for a single white dwarf.

Key words: binaries: symbiotic – circumstellar matter – scattering – polarization – stars: individual: Z And

1. Introduction

Since the discovery of the occurrence of Raman scattering in symbiotic systems (Schmid 1989) an additional observational tool has become available which potentially allows to probe the binary orbits and interbinary nebular material in new detail. In this paper we present for Z And a series of spectropolarimetric observations of the Raman scattered emission lines $\lambda\lambda$6825,7082 and determine orbital parameters which in turn lead to better estimates of the stellar masses. Z And is a prototypical symbiotic system with one of the most comprehensive records of photometric and spectroscopic observations (e.g. Fernandez-Castro et al. 1988, 1995; Mikolajewska & Kenyon 1996; see also Kenyon 1986, and references therein). Despite this wealth of data, very basic questions about the physical nature of the system remain open. In the paper by Mikolajewska & Kenyon (1996) the current knowledge and its limitations are nicely summarized and will not be repeated here in detail. Apart from the poorly determined stellar masses there remains the interesting and fundamental question of whether the hot component is a white dwarf or an accreting main sequence star.

Send offprint requests to: hschmid@lsw.uni-heidelberg.de (H.M. Schmid), or hschild@astro.phys.ethz.ch (H. Schild)

⋆ Based on observations obtained with the William Herschel Telescope of the Royal Greenwich Observatory, La Palma, Canary Islands

Below, we present after a short description of the observations, the observed flux and polarization variations of the Raman features which we then discuss in terms of the binary orbit. An attempt is then made to constrain the mass of the hot component with the inclination derived from the polarimetric data and a mass function given by Mikolajewska & Kenyon (1996).

2. Observational data

In the framework of a spectropolarimetric monitoring program of a number of northern symbiotic stars, we obtained a sequence of observations of Z And with the 4.2m William Herschel Telescope and the ISIS spectrograph. The data were collected by RGO support astronomers as service observations. Observing dates are summarized in Table 1 and further observational details can be found in previous papers of this series (Schmid & Schild 1994, 1997; Schild & Schmid 1996, 1997).

The phase in Table 1 is calculated according to the photometric ephemeris of Formiggini & Leibowitz (1994):

$$\mathrm{Min(vis)} = \mathrm{JD}\,2442666(\pm 10) + 758.8(\pm 2)\,E\,. \quad (1)$$

Radial velocity measurements revealed for the cool giant an orbital motion with the same period. The times of spectroscopic conjunction, i.e. when the cool component is closest to us, coincides accurately with photometric minima (Mikolajewska & Kenyon 1996).

Because the orbital period of Z And is close to 2 years, our observations are clumped at phases just prior to quadrature.

2.1. Line flux and spectroscopic structure

In Table 1 we list equivalent widths (EW) for the Raman line λ6825. The red giant continuum at λ6825 shows only little spectral structure which can be removed with a suitable comparison star (BS8942). We estimate the accuracy of the EW(λ6825) to be about 5%. According to Table 1 the equivalent widths of λ6825 show small, but significant, fluctuations on the $\pm$10% level. The fluctuations are not obviously linked to the orbital phase.

During our observing period, Z And was in a quiescent state with possibly periodic variations of about $0.2 - 0.3$ mag in the

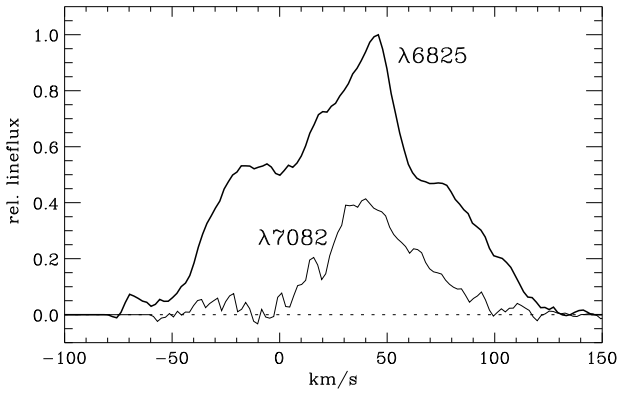

Fig. 1. Profiles for the Raman lines λ6825 and λ7082 in the velocity space of the original O VI lines. The plotted profiles are means of all our observations (except observation 001).

Table 1. Log of spectropolarimetric observations and emission line equivalent widths for λ6825.

Obs.	date	$JD_{244...}$	phase	$EW_{\lambda6825}$
001	19-08-1991	8487.53	7.672	9.3
302	27-10-1992	8922.54	8.245	7.9
506	22-07-1993	9190.70	8.599	8.9
704	23-08-1993	9222.56	8.641	8.3
1004	19-09-1994	9614.65	9.157	10.4
1104	28-10-1994	9648.55	9.202	9.6

visual range (Formiggini & Leibowitz 1994; Skopal et al. 1995) and less for longer wavelengths (Taranova & Yudin 1981). We may thus conclude that the λ6825 line flux varied less than about $\pm$20 %. This is in agreement with the measurements of Mikolajewska & Kenyon (1996) who measured in the 1994/1995 season for λ6825 a mean line flux of $F = 4.5 \cdot 10^{-12}$ erg cm^{-2} s^{-1} with a scatter of $\sigma = \pm 15$ %.

For all observing dates a constant line flux ratio $F(\lambda6825)/F(\lambda7082) = 3.6$ is determined within the estimated measuring uncertainty of about 20%.

Fig. 1 shows the mean line structure of the Raman lines. The λ6825 profile shows a central peak with a weaker component on each side. In the λ7082 component the blue component is absent and also the red component is barely visible. The λ7082 component coincides with a strong TiO band which makes the subtraction of the stellar continuum difficult. It is not clear whether the remaining structure in the blue wing of λ7082 is due to inaccurate subtraction of the stellar continuum or whether it is due to additional TiO absorption in the extended atmosphere.

We note that the blue component of the λ7082 feature is in many symbiotic systems relatively weak when compared to the λ6825 line structure.

2.2. Observed Raman line polarization

The Raman lines produce a strong polarization signal. The continuum polarization p_c,γ_c is small and wavelength independent in the spectral range covered (6730Å– 7190Å). Within the errors, p_c,γ_c is the same for all our observations. We measure $p_c = 1.20 \pm 0.04$ % and $\gamma_c = 46.9 \pm 1.2°$, where the uncertainties are the one-sigma deviations between our 6 measurements. This value is in good agreement with the polarimetric data of Schulte-Ladbeck (1985). We conclude as in Schmid & Schild (1994) that the observed continuum polarization in Z And is mainly interstellar in origin.

In order to obtain the intrinsic line polarization we have to correct for the interstellar polarization and to subtract the stellar continuum emission (see e.g. Schmid & Schild 1994). Fig. 2 shows the resulting spectropolarimetric line structure for the λ6825 component for all our observations. The panels give the intensity I, the "rotated" Stokes parameters Q'_ℓ and U'_ℓ, the percentage polarization p_ℓ and the polarization angle γ_ℓ. Q'_ℓ and U'_ℓ are the Stokes parameters in a coordinate system which has been aligned with the mean polarization angle $\langle\gamma\rangle$ in the λ6825 Raman line. This means, that the U'_ℓ-parameter integrated over the entire λ6825 feature is zero. The mean position angle $\langle\gamma\rangle$ is indicated in the panels.

The flux weighted mean percentage polarization p_ℓ and mean polarization angle γ_ℓ for the λ6825 and λ7082 components are listed in Table 2. For the λ6825 component the same parameters are given for four wavelength bins of 5 Å widths corresponding to the extreme blue, blue, red and extreme red portion of the line. A comparison between the Raman lines λ6825 and λ7082 shows that the polarization signal behaves very similar in both components.

3. Polarization variation and orbit

3.1. General

The production of the Raman lines in symbiotic stars is explained by a scattering geometry where strong O VI radiation is produced in the ionized region near the hot component and converted by neutral hydrogen into Raman photons in the extended atmosphere and wind of the cool giant (Schmid 1992,1996; Schmid & Schild 1994; Harries & Howarth 1997; Lee & Lee 1997). Such a scattering geometry rotates relative to the line of sight due to the binary motion. Therefore, a phase locked rotation of the polarization angle is expected. For an inclined orbit the rotation rate is fast near conjunction and slow near quadrature. In addition the percentage polarization is predicted to vary periodically. Polarization minima are expected near conjunction because the binary configuration is closest to a forward or backward scattering situation. The highest polarization will occur at quadratures when the binary situation is optimal for right angle scatterings.

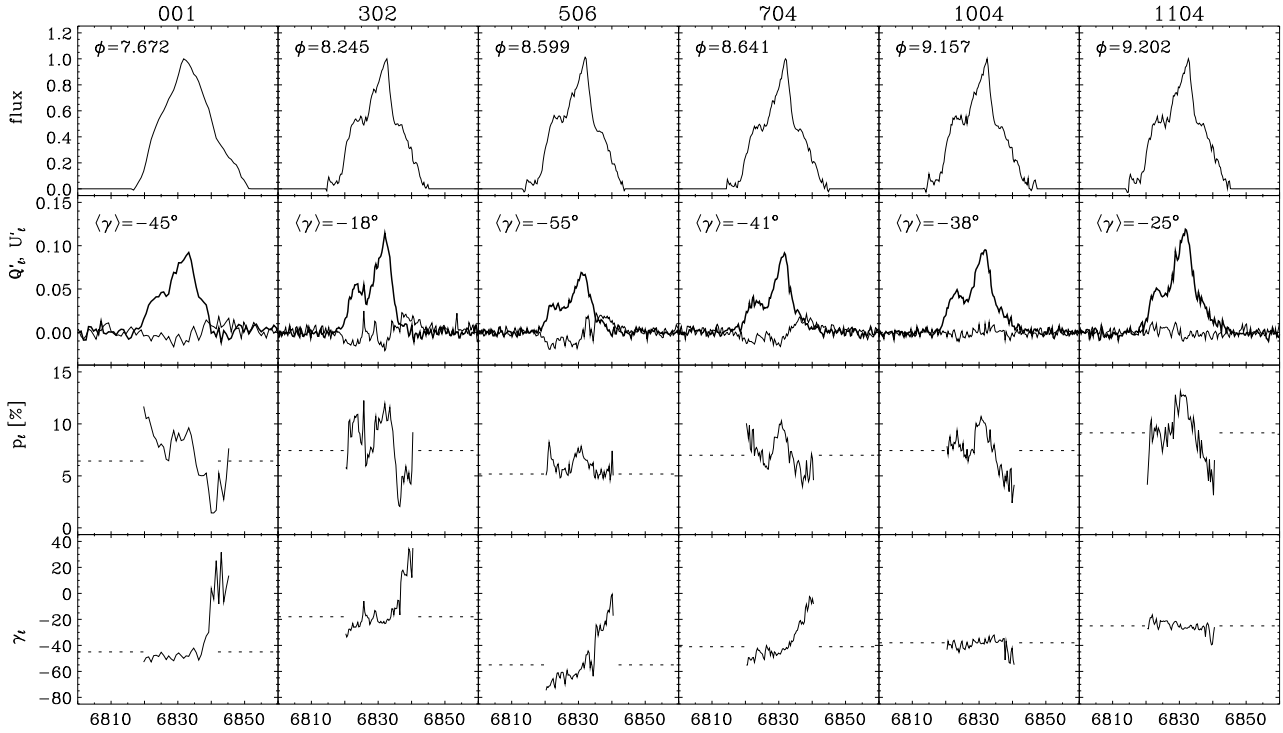

Fig. 2. Normalized flux I, rotated Stokes parameters Q'_ℓ (bold) and U'_ℓ, percentage polarization p_ℓ and position angle γ_ℓ for the λ6825 line in Z And for all our WHT observations. The alignment of the $Q' - U'$ system (for each individual measurement) is equal to the flux weighted mean of the polarization angle $\langle\gamma\rangle$ as indicated in γ_ℓ by a dashed line. Thus, the integrated U'-parameter vanishes in that system. The dashed line in the p_ℓ-panels gives the (flux weighted) mean percentage polarization.

Table 2. Flux weighted polarization in the integrated (total) λ6825 and λ7082 lines. Also given are for the λ6825 component the values for 4 subintervals corresponding to the extreme blue, blue, red, and extreme red portions of the line.

Obs.	$\lambda6825_{\rm total}$		[6820–6825]		[6825–6830]		[6830–6835]		[6835–6840]		$\lambda7082_{\rm total}$	
	p_ℓ	γ_ℓ	p_ℓ	γ_ℓ	p_ℓ	γ_ℓ	p_ℓ	γ_ℓ	p_ℓ	γ_ℓ	p_ℓ	γ_ℓ
001	6.43	135	9.0	131	8.1	132	8.7	133	4.9	139	6.03	130
302	7.43	162	9.8	156	9.0	162	9.5	160	3.6	16	7.43	162
506	5.18	125	6.0	113	6.1	117	6.5	126	5.0	157	5.18	125
704	7.00	139	7.9	131	7.4	134	8.4	138	5.2	161	7.22	143
1004	7.43	141	8.0	140	8.0	141	9.1	143	5.0	140	7.43	141
1104	9.14	155	8.5	158	9.9	157	11.3	154	6.8	152	7.76	150

3.2. Orbit inclination and orientation

In Z And, the polarization signal in the Raman lines shows indeed the typical phase locked variations. The polarization angle rotates counter-clockwise and steadily with phase and the percentage polarization increases towards the quadrature phases (Fig. 3, Table 2). This behaviour is particularly well visible in the blue portion of the λ6825 component. Theoretical models and previous observations suggest that the orbital motion is best reflected in the blue wing of the Raman lines. The reason for this is that these photons originate predominately from scatterings close to the binary axis where the scattering H^0-atoms in the giant's wind move towards the O VI photon source and introduce a blueward Doppler shift. The photons in the red line wing originate from the receding (relative to the O VI source) outer part of the red giant wind, which is geometrically less well defined and where geometric cancellation of the polarization signal is important (see e.g. Schmid & Schild 1994,1997).

The orbit inclination for Z And can be estimated from the variation in the percentage polarization. For this, we assume that the line polarization can be described by the simple relation

$$p = p_{\rm max} \sin^2\alpha\,, \qquad (2)$$

where α is the angle between the line of sight and the binary axis connecting the two stars. This approximation is supported

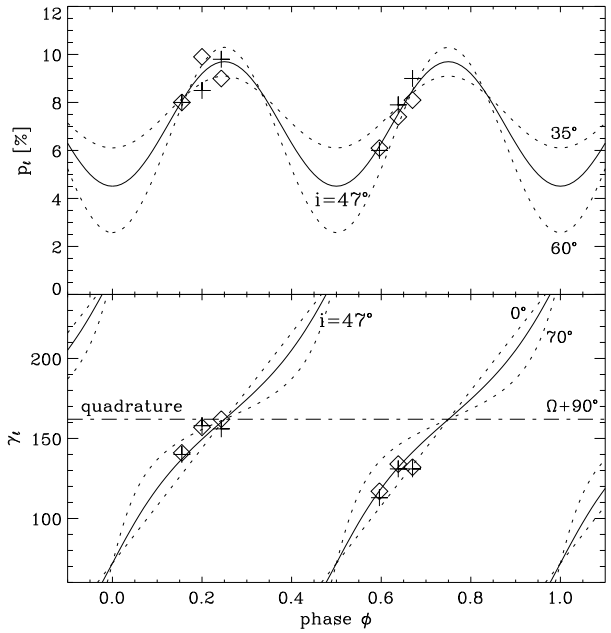

Fig. 3. Measured percentage polarization p_ℓ and polarization angle γ_ℓ as function of phase ϕ for the blue (diamonds) and extreme blue (crosses) portion of the Raman line λ6825. The solid lines is the fit solution $i = 47°$, $\Omega = 72°$ and the dotted curves illustrate the uncertainty for i.

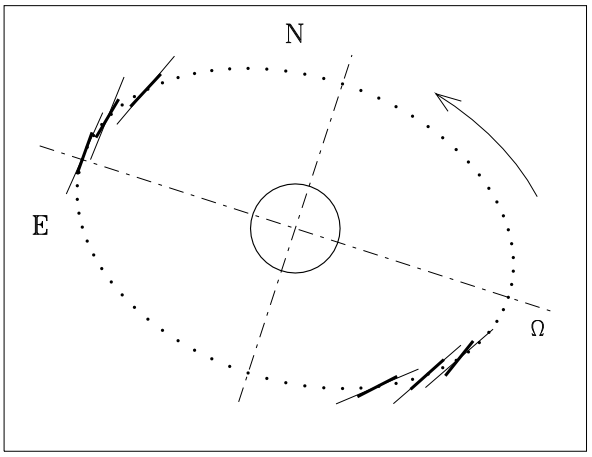

Fig. 4. Polarimetric orbit ($\Omega = 72°$, $i = 47°$) of Z And for the extreme blue portion of the λ6825 feature. The position of the hot component relative to the cool giant (central circle) is given by dots at $\varphi = 5°$ intervals. Short thick lines show the calculated polarization directions at the times of observations, and long thin lines the measured polarization direction.

by model calculations (Schmid 1996; Harries & Howarth 1997) and observations of the eclipsing system HBV 475 (Schild & Schmid 1997) which show such a simple $\sin^2\alpha$-like behaviour. The above relation can also be expressed in terms of the orbital phase angle $\varphi = 360° \cdot \phi$ and the inclination i (see Eq. 7 in Schmid 1992)

$$p = p_{\max}\,(\cos^2\varphi\cos^2 i + \sin^2\varphi)\,, \tag{3}$$

where the orbital phase is given by the photometric phase (Eq. 1).

A least square approximation of relation (3) to the p_ℓ [6820–6825] data points (extreme blue part of the Raman line) yields the solution $i = 47°$, $p_{\max} = 9.7\%$ and a standard deviation of $\sigma = 0.4\%$. Practically identical values are obtained for the p_ℓ [6825–6830] data points ($i = 47°$, $p_{\max} = 9.6\%$, $\sigma = 0.4\%$).

We estimate uncertainty ranges of $35° - 60°$ for i and $9.1\% - 10.3\%$ for $p_{\max}$. The best fit solution and dotted curves illustrating the uncertainty range are plotted in Fig. 3. This figure also illustrates that a better phase-distribution of data points could improve substantially the accuracy of the i determination.

The orientation of the orbital plane for Z And can be determined from the measured polarization angles. For this, we assume that the polarization in the blue wing of the Raman lines is perpendicular to the binary axis. Thus, the orientation of the line of nodes Ω may be determined by the polarization angle in the blue line wing at quadrature phase. The observations 302 were taken very close to quadrature phase and suggest an angle close to 70° for Ω. A better estimate is possible with a least square solution to all data points. Therefore, we use the relation

$$\gamma = \mathrm{atan}\left(\frac{\sin\varphi}{\cos\varphi\cos i}\right) + \Omega \tag{4}$$

for the polarization angle. This relation is a rotated (90°) description of the position angle of the binary axis for an inclined binary system with an orbit of zero eccentricity.

The least square solution for the polarization angles in the extreme blue portion ([6820–6825]) of the Raman line gives $\Omega = 72°$ and $i = 43°$ with a standard deviation of $\sigma = 6°$. The best solution for the blue portion of the line ([6825–6830]) $\Omega = 75°$, $i = 40°$, and $\sigma = 5°$ is not significantly different.

The uncertainty in the Ω-determination is about $\pm 6°$. The resulting inclination confirms the result from the fit to the percentage polarization. However, the inclination dependence of the $\gamma(i, \phi)$-curves is very small for small inclinations and the least square solution which we found can only be considered as an upper limit $i \lesssim 65°$. We prefer therefore the i-estimate ($i = 47°$) from the percentage polarizations. Fig. 3 shows the fit solution for $\Omega = 72°$ and $i = 47°$, together with dotted curves for the inclinations $i = 0°$ and 70°.

Fig. 4 gives a geometric representation of the spectropolarimetric orbit as projected onto the sky. Note, that spectropolarimetric data are invariant to a 180°-rotation of the scattering geometry. Thus the orbit plotted in Fig. 4 could also be rotated by 180° on the celestial sphere which leaves an ambiguity in the position of the ascending and descending nodes but does not change the orientation of the line of nodes.

3.3. Mass of the hot component

The mass function $m_{\rm f}$ as derived from radial velocity measurements of the red giant is 0.024 ± 0.005 $M_\odot$ (Mikolajewska & Kenyon 1996) and can be written as

$$m_{\rm f} = \frac{(M_{\rm h} \sin i)^3}{M_{\rm sys}^2} ,$$

where $M_{\rm h}$ stands for the mass of the hot component and $M_{\rm sys}$ for the total system mass. The mass of the hot component is thus

$$M_{\rm h} = 0.288 \, \frac{M_{\rm sys}^{2/3}}{\sin i} ,$$

For the estimate of $M_{\rm h}$, a relative error of about ± 20 % is introduced by the uncertainty in the determination of i and in addition about ± 10 % from the mass function. Further, we have to consider the dependence of $M_{\rm h}$ on the total system mass. Determinations of $M_{\rm sys}$ for symbiotic systems (e.g. Mikolajewska & Kenyon 1992; Schmutz et al. 1994; Schild et al. 1996) suggest a typical value of $M_{\rm sys} \approx 1.8$ $M_\odot$. Taking a system mass between 1.3 and 2.3 $M_\odot$ thus leads to a hot components mass of

$$M_{\rm h} = 0.65 \pm 0.28 \ M_\odot$$

Such a mass is typical for white dwarfs and indicates that the hot sources luminosity is due to thermonuclear reactions rather than accretion onto a main sequence star.

4. Discussion

Time series of the Raman polarization which cover more than one orbital period have currently been reported for the symbiotic systems: SY Mus (Harries & Howarth 1996), AG Dra (Schmid & Schild 1997) and HBV 475 (Schild & Schmid 1997). Here we add a further object, Z And, which brings the count of reasonably well studied symbiotics to four, all of which are of S–type. In all systems it has been demonstrated that the Raman polarization is locked to the orbital phase i.e. the rotation of the polarization angle is closely linked to the orbital motion. In HBV 475 and Z And there is also a clear relationship between the percentage polarization and the orbital phase. As predicted by numerical scattering models (Schmid 1996; Harries & Howarth 1997) polarization maxima occur at quadrature phases and minima at conjunction phases. The overall assumptions of these models, namely that the O VI emission and the H^0 scattering regions are aligned with the binary axis and closely associated with the stellar hot and cool components are strongly confirmed by these observations. Such an irradiation and scattering geometry seems to be common among at least symbiotic S–types.

Since the temporal changes of the polarization in the Raman lines are dominated by the binary orbit, otherwise unobservable parameters like the orbital inclination and orientation on the celestial sphere can directly be measured. In the case of Z And, we find an inclination of $i = 47 \pm 12^\circ$ and an orbit orientation $\Omega = 72 \pm 6^\circ$.

Accurate orbital parameters are required to measure the mass of stellar components. By assuming a total system mass in a plausible range we find that the hot component in Z And has a mass which is typical for single white dwarfs.

Acknowledgements. We are indebted to the La Palma support astronomers who carried out the service observations. We are particularly grateful to René Rutten and Vik Dhillon. We thank Urs Mürset, Harry Nussbaumer and Werner Schmutz for valuable discussions and comments on the manuscript. This work was financially supported by the Swiss National Science Foundation.

References

Fernandez-Castro T., Cassatella A., Gimenez A., Viotti R., 1988, ApJ, 324, 1016
Fernandez-Castro T., Gonzalez-Riestra R., Cassatella A., Taylor A.R., Seaquist E.R., 1995, ApJ, 442, 366
Formiggini L., Leibowitz E.M., 1994, A&A, 292, 534
Harries T.J., Howarth I.D., 1996, A&A, 310, 235
Harries T.J., Howarth I.D., 1997, A&AS, 121, 15
Kenyon S.J., 1986, The Symbiotic Stars, Cambridge Univ. Press, Cambridge
Lee H.W., Lee K.W., 1997, MNRAS, 287, 211
Mikolajewska J., Kenyon S.J., 1992, AJ, 103, 579
Mikolajewska J., Kenyon S.J., 1996, AJ, 112, 1659
Schild H., Schmid H.M., 1996, A&A, 310, 211
Schild H., Schmid H.M., 1997, A&A, in press
Schild H., Mürset U., Schmutz W., 1996, A&A 306, 477
Schmid H.M., 1989, A&A, 211, L31
Schmid H.M., 1992, A&A, 254, 224
Schmid H.M., 1996, MNRAS, 282, 511
Schmid H.M., Schild H., 1994, A&A, 281, 145
Schmid H.M., Schild H., 1997, A&A, 321, 791
Schmutz W., Schild H., Mürset U., Schmid H.M., 1994, A&A, 288, 819
Schulte-Ladbeck R., 1985, A&A, 142, 333
Skopal A., Hric L., Chochol D., et al., 1995, Contrib. Astron. Obs. Skalnate Pleso, 25, 53
Taranova O.G., Yudin B.F, 1981, Sov. Astron., 25, 710

This article was processed by the author using Springer-Verlag LaTeX A&A style file *L-AA* version 3.